Artificial maturation of [FeFe] hydrogenase in a redox polymer film

Supplementary information

Christina Felbek, Steffen Hardt, Cécilia Papini, Debajyoti Pramanik, Vincent Artero, Marc Fontecave, Vincent Fourmond, Nicolas Plumeré, Christophe Léger

Methods

Polymer synthesis. Polyvinyl alcohol (PVA) (1 g) was dissolved in water (19 ml) precipitated from an acetone/methanol mixture (40 mL). The solid was dried overnight at 60 °C under vacuum. PVA (0,12 g) and 1-(2-(((6-Isocyanatohexyl)carbamoyl)oxy)ethyl) -1'-methyl-[4,4'-bipyridine]-1,1'-diium bromide iodide (0.08 g; 0.14 mmol) were dissolved in N-methyl-2-pyrrolidone (NMP) by sonication. Dibutyltin dilaurate (20 µL) was added and the mixture was stirred at RT for 24 h. The polymer was precipitated from EtOAc and dried under vacuum. The crude product was dissolved in dist. water and purified via Viva Spin centrifugation (5 kDa). This synthesis was essentially the same as that described in refs [1,2].

^{1}H-NMR (400 MHz, DMSO-d_6): d_H (ppm): 9.15 (d, J= 6.4 Hz, V^{2+}); 9.06 (d, J= 6.5 Hz, V^{2+}); 8.63-8.45 (m, V^{2+}); 4.99 (s); 4.49 (s); 4.00 (broad multiplet, PVA); 2.99 (broad multiplet, PVA); 2.18-1.02 (broad multiplet, PVA).

Film preparation.

MET

Anaerobic conditions. The polymer/hydrogenase films discussed in the first part of the manuscript were prepared by letting dry for 24 hours, onto the surface of the rotating disc glassy carbon electrode as well as its plastic support (0.28 cm^2, including glassy carbon surface), either 0.5 µL of a 25 µM solution of apo-enzyme and 1.5 µL of polymer (6 g/L), or 0.5 µL of a 25 µM solution of apo-enzyme, and 1.5 µL of polymer (6 g/L) containing a small amount (about 0.2 pmol) of holo-enzyme. These two methods give thin and thick films, respectively. For the optimisation and examination of the effect of exposure to oxygen, thick films were prepared with the latter procedure, except that the drying time was 2h or 5h (Fig. S9).

Aerobic conditions. The films were prepared like under aerobic conditions: with or without a small amount of holo enzyme, in the glove box, dried under anaerobic conditions for ten minutes (during which catalytic oxidation of H_2 and reduction of the viologen appears to stabilize the film, as discussed in main text), exposed to air at 4°C for two hours, and reintroduced in the glove box to monitor the maturation under anaerobic conditions. The results are shown in Fig. S10 (maturation), and S11 (non catalytic voltammetry under argon after maturation), and as a dotted blue line in main text Fig. 1 (thick film prepared with a small amount of holo enzyme and exposed to air).

DET

Anaerobic conditions. For DET electrochemistry experiments, the films were obtained by letting dry 2 min 0.5 µL of a solution of apo *Me* hydrogenase (25 µM in pH 7 phosphate buffer) onto a 0.07 cm^2 rotating disc glassy carbon electrode.

Aerobic conditions. The films were prepared as described for anaerobic conditions: The solution of the apo *Me* hydrogenase was equilibrated with air and kept at 4°C. After 40 min and 2h (figs S9 and S10), 0.5 µL of the solution were at each time reintroduced in the glove box, spread on the electrode surface and dried 2 min to finally monitor the maturation in the electrochemical set-up.

Electrochemistry. The electrochemicals set-up that we use has been described before[3]. The concentration of H_2 was varied by mixing pure H_2 with Ar in an Aalborg gas proportioner, and bubbling the mix directly into the electrochemical cell solution containing a mixed buffer (MES, HEPES, sodium acetate, TAPS, CHES, 5 mM) and NaCl (0.1M).

Electrochemical determination of the Michaelis constant by taking into account hydrogen depletion at the film/solution interface. Figure S7 shows the catalytic current *i* against the bulk concentration of H_2, $[H_2]_\infty$; each series of data points corresponds to a series of electrode rotation rates (ω): the lower ω, the lower the current *i*, which indicates substrate depletion at the film/solution interface. The interfacial concentration $[H_2]_0$ equates $[H_2]_\infty - i/(\alpha\sqrt{\omega})$, where the value of α is unknown, but it can be determined by fitting, by assuming that its best value makes the plot of *i* against calculated $[H_2]_0$ the smoother. The corresponding QSoas[4] code (for QSoas version 2.2 and above) is included below.

Measurements of the activation time constants and estimation of film stability

Analysis of the data in Fig. 1 and S5A with an equation that takes into account film loss, simply by multiplication of the theoretical equation $i_\infty(1-\exp(-t/\tau))$ by an exponential decay, as explained in ref 5. The QSoas command is `fit-exponential-decay /loss=true`. We typically obtained time constants of film loss of 30 min (thin film) and 5 h (thick film). The data in ref [6] shows more stable currents, but they were recorded at lower T (RT instead of 40°C in our experiments).

QSoas code for the determination of K_m from electrochemical experiments in which the depletion of H_2 near the electrode surface is significant

Build the file `data.dat` with 5 columns: $[H_2]_\infty$, time, current, omega and normalized current (obtained by dividing by a baseline)

Edit the file run.cmd:

```
unflag flagged
load data.dat
set-meta alpha ${1} ! the guessed value of alpha is input as a parameter
apply-formula y=y5 ! normalized current
apply-formula x=x-y2/(${1}*sqrt(y4)) ! calculate [H2]_0 using the value of the current (y2), alpha and omega (y4), considering that i \propto \sqrt(\omega) \times ([H2]_infty-[H2]_0)
sort
strip-if x<0
```

```
auto-filter-bs
S 0 1 ! calculate the difference between signal and filtered signal to estimate roughness
stats /meta=alpha /accumulate=alpha,y_norm ! accumulate the values of alpha and y_norm into a dataset
```

Then run:

```
run-for-each /range-type=lin run.cmd 1e-6..13e-6:100 /silent=true
pop ! this outputs the roughness against alpha, the minimum gives the best value of alpha
```

Then run

```
@ runl.cmd xxx ! replace xxx with the best value of alpha
```

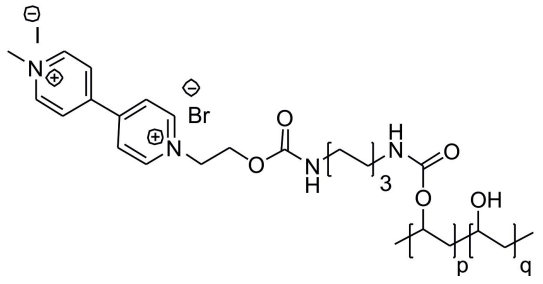

Fig. S1: Structure of the 4,4´-methylviologen redox polymer

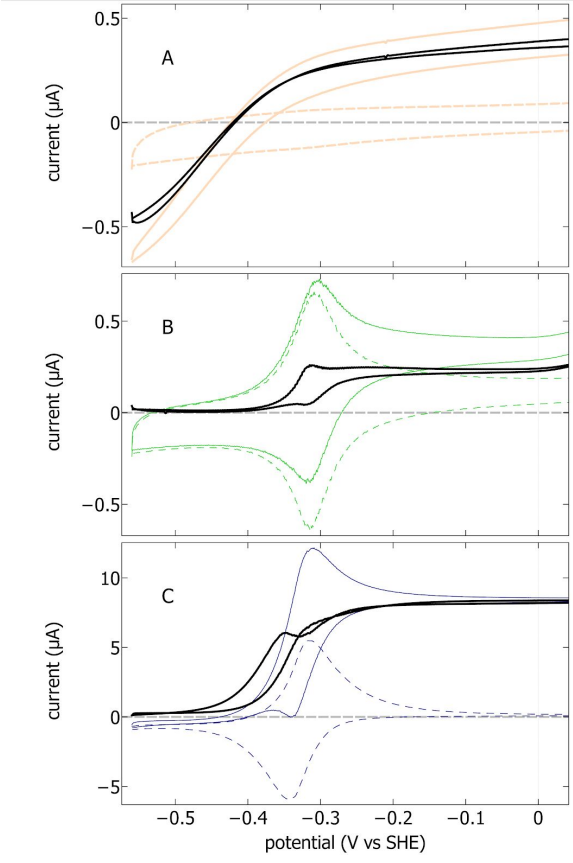

Figure S2 : Comparison of the catalytic waveshapes (black) of the maturated hydrogenase films from Fig 1.
Panel A: standard catalytic response under DET conditions (obtained after subtraction of the background current (orange dashed line) recorded with no enzyme), which can be directly compared to that published in ref [7]. Panel B: catalytic response (black), obtained by subtracting the non-catalytic signal recorded under argon (green dashed line) from the catalytic signal recorded under H_2 (green solid line), under conditions of MET in a thin polymer/hydrogenase film.
Panel C: same as panel B, but for conditions of MET in thick polymer/hydrogenase film.
In panels B and C the subtraction essentially removes the contributions from the electrode and from the viologen.
In all cases: scan rate 20 mV/s, 40 °C, pH 7, 1 atm. H_2, electrode rotation rate 3000 rpm.

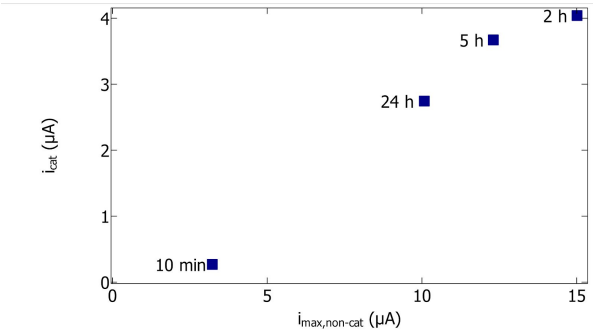

Fig. S3: correlation of film thickness (maximal non catalytic peak current at 200mV/s) and final maturation current (at -160 mV) of thick (anaerobic) hydrogenase/polymer films with different drying times (see time period indicated left of each data point). In all cases: 40 °C, pH 7, 1 atm. H_2, 2000 rpm.

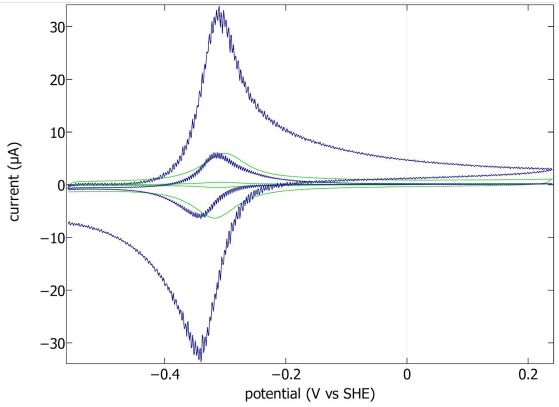

Fig. S4. Non catalytic voltammetric signals of the two hydrogenase / polymer films after the maturation experiments shown in Fig. 1, recorded under Ar, at 20 and 200 mV/s. The thin and thick film CVs are shown in green and dark blue, respectively (same color code as in main text figure 1).

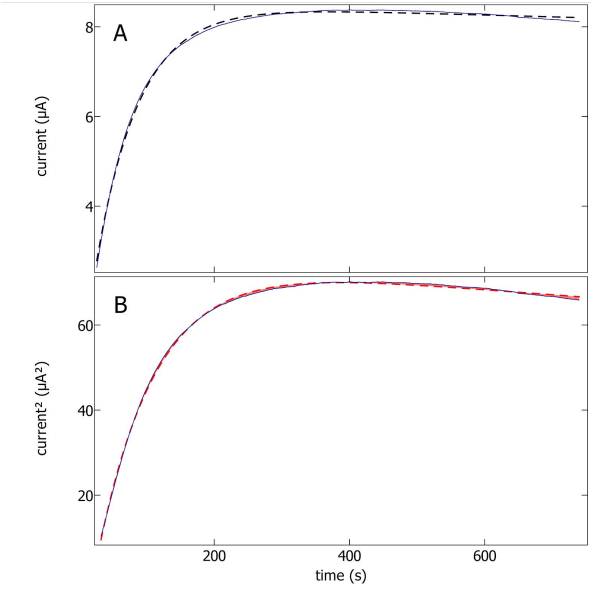

Fig. S5. Determination of the time constant of activation with the apo-hydrogenase embedded in a thick hydrogenase/polymer film under MET conditions.
Panel A: H_2 oxidation current (dark blue) resulting from the maturation in a thick film under conditions of MET. An exponential decay (dashed black line) was fitted to the current as described in the first part of the methods section.
Panel B: square of the maturation current (dark blue) and the corresponding exponential fit (dashed red line). Note that plotting the square of the current artificially enhances the visual effect of film desorption.

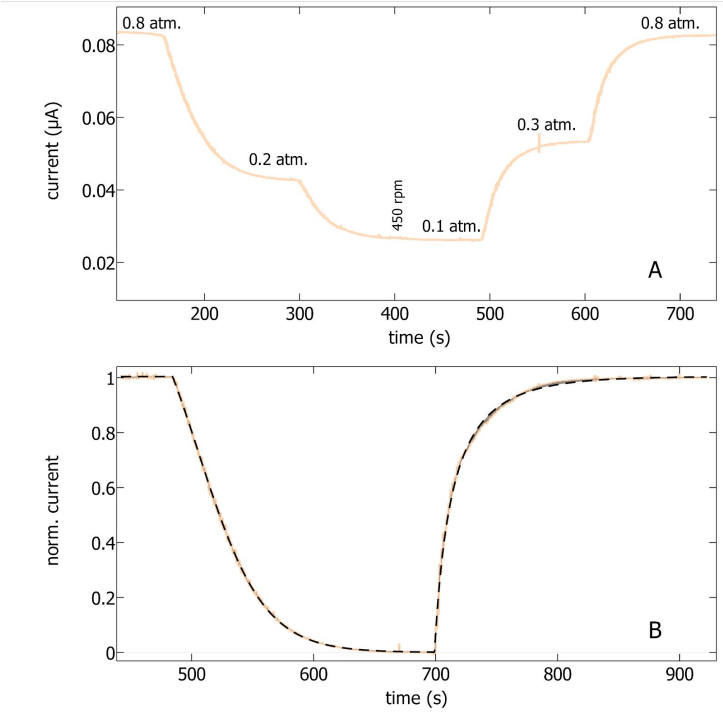

Fig. S6: Experiments to measure the K_m of maturated *Me* hydrogenase under DET conditions, at pH 7, 5°C, 2000 rpm.
Panel A: the current is recorded as a function of time, and the H_2/N_2 mix is varied to obtain different partial pressures of H_2. The values of the asymptotic current are plotted against $[H_2]$ in main text figure 3C. The change in rotation rate at 400s makes no difference, showing that depletion is negligible, therefore no correction of $[H_2]_0$ is needed.
Panel B: Change in current against time in an experiment where 100% H_2 is flushed away by Ar (from t = 480 s) and then reintroduced into the electrochemical cell (at 700 s). The fit of the model described in ref [8] is shown as a black dashed line, and returned a value of K_m = 0.45 atm. H_2.

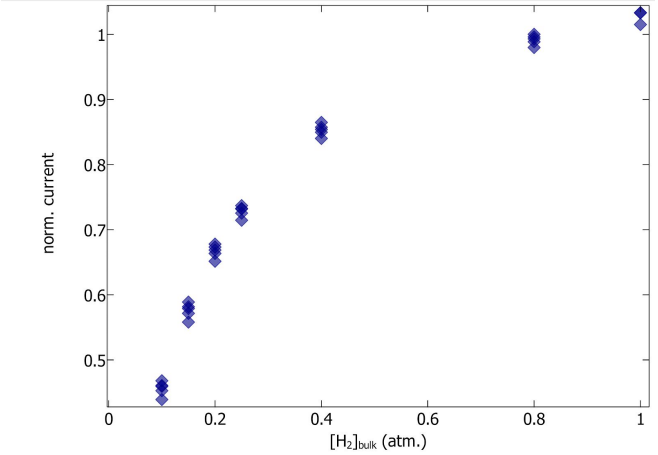

Fig. S7: I against $[H_2]_\infty$ in the experiment performed with the thick hydrogenase/polymer film. At each H_2 concentration, the current was measured at 4 rotation rates, 2567, 2066, 1570 and 860 rpm.

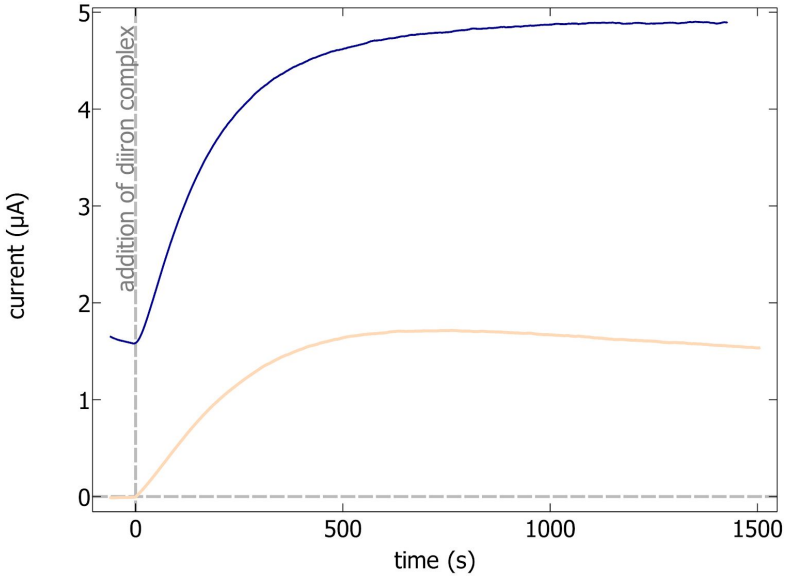

Fig. S8: Comparison of the electrochemically-monitored time-resolved artificial maturation of films of *Me* apo-hydrogenase: thick film under MET conditions (dark blue), versus DET conditions (orange) **at 30°C.** Fitting the square of the current (MET conditions) or to the current (DET conditions) gave activation time constants of 220 s and 250 s, respectively. In all experiments, the maturation is detected as an increase in hydrogen oxidation current after 53 nM $[Fe_2(adt)(CO)_4(CN)_2]^{2-}$ is added to the electrochemical cell, at t=0 s. Electrode potential E=-160mV vs SHE, pH 7, 1 atm. H_2, electrode rotation rate ω = 2000 rpm.

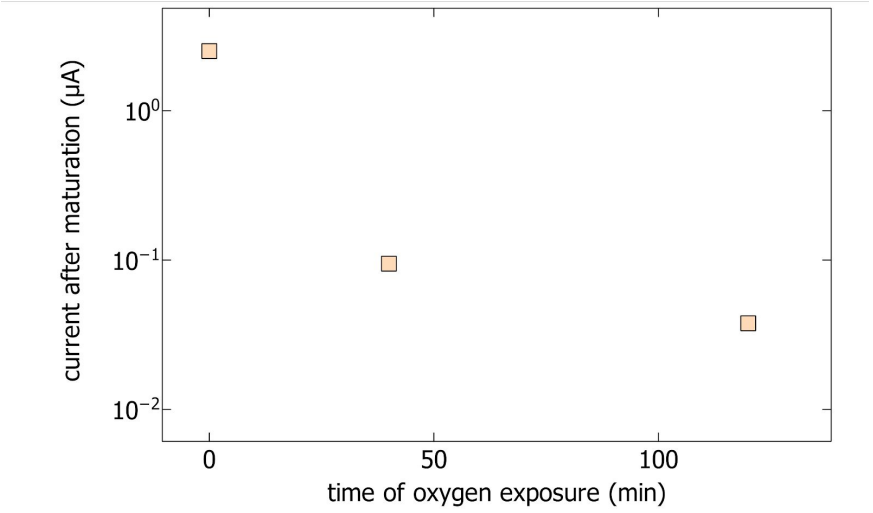

Fig. S9: Final catalytic current after maturation (under DET conditions) of films of a solution of apo *Me hydrogenase* that has been exposed to air (see procedure in methods section) for different time periods.

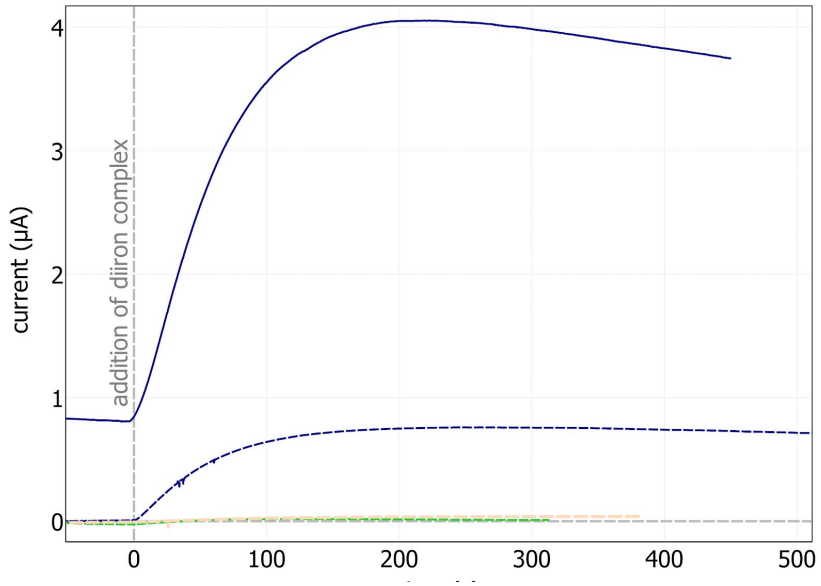

Fig. S10. Electrochemically-monitored time-resolved artificial maturation of films of *Me* apo-hydrogenase dried for 2 h either under anaerobic conditions (solid dark blue line) or under air under three distinct conditions (dashed line): MET in a thin polymer film (green) or in a thicker polymer film (dark blue), and DET (orange) see procedures in the above methods.
In all experiments, the maturation is detected as an increase in hydrogen oxidation current after 53 nM $[Fe_2(adt)(CO)_4(CN)_2]^{2-}$ is added to the electrochemical cell, at t=0 s. Electrode potential E=-160mV vs SHE, T=40°C, pH 7, 1 atm. H_2, electrode rotation rate ω = 2000 rpm.

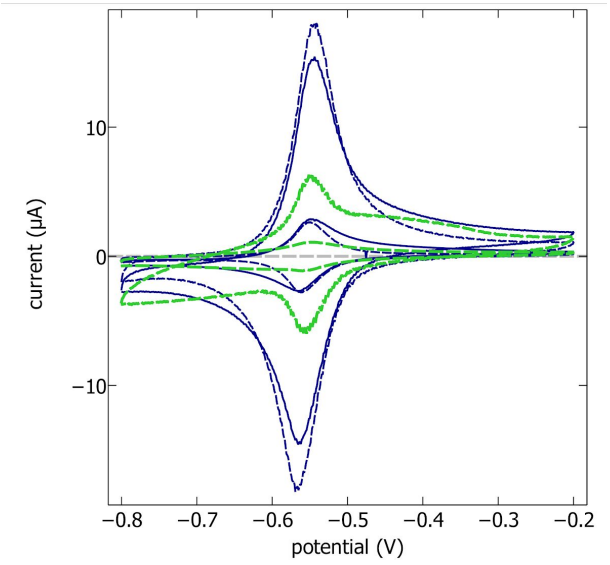

Fig. S11: Non catalytic voltammetric signals of the three hydrogenase / polymer films discussed in Fig. S7, dried for 2h, recorded under Ar under MET conditions, at 20 and 200 mV/s. The CVs of the thin and thick hydrogenase/polymer films are shown in green and dark blue, respectively (same color code as in figure S7).

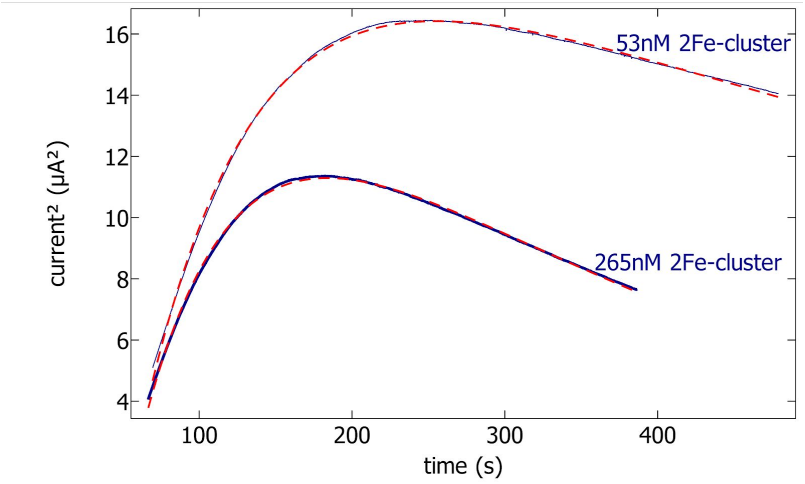

Fig. S12: Square of the maturation current (dark blue line) of apo-hydrogenase embedded in a thick polymer film (dried 2h in the glove box) against time in the presence of different concentrations of the dinuclear complex $[Fe_2(adt)(CO)_4(CN)_2]^{2-}$. The concentration was increased 5 fold (thick dark blue line) compared to the concentration in a standard experiment (thin dark blue line). Exponential fits (red dashed lines) gave the same time constant (83s) for both experiments but with different time constants of film loss (53nM: 900s, 265nM 350s). Note that plotting the square of the current artificially enhances the visual effect of film desorption.

References

1 E. A. Appel, X. J. Loh, S. T. Jones, F. Biedermann, C. A. Dreiss and O. A. Scherman, *J. Am. Chem. Soc.*, 2012, **134**, 11767–11773.

2 F. Biedermann, E. A. Appel, J. del Barrio, T. Gruendling, C. Barner-Kowollik and O. A. Scherman, *Macromolecules*, 2011, **44**, 4828–4835.

3 C. Léger, S. Dementin, P. Bertrand, M. Rousset and B. Guigliarelli, *J. Am. Chem. Soc.*, 2004, **126**, 12162–12172.

4 V. Fourmond, *Anal. Chem.*, 2016, **88**, 5050–5052.

5 V. Fourmond, T. Lautier, C. Baffert, F. Leroux, P.-P. Liebgott, S. Dementin, M. Rousset, P. Arnoux, D. Pignol, I. Meynial-Salles, P. Soucaille, P. Bertrand and C. Léger, *Anal. Chem.*, 2009, **81**, 2962–2968.

6 A. A. Oughli, S. Hardt, O. Rüdiger, J. A. Birrell and N. Plumeré, *Chem. Commun.* , 2020, **56**, 9958–9961.

7 G. Caserta, C. Papini, A. Adamska-Venkatesh, L. Pecqueur, C. Sommer, E. Reijerse, W. Lubitz, C. Gauquelin, I. Meynial-Salles, D. Pramanik, V. Artero, M. Atta, M. Del Barrio, B. Faivre, V. Fourmond, C. Léger and M. Fontecave, *J. Am. Chem. Soc.*, 2018, **140**, 5516–5526.

8 V. Fourmond, C. Baffert, K. Sybirna, S. Dementin, A. Abou-Hamdan, I. Meynial-Salles, P. Soucaille, H. Bottin and C. Léger, *Chem. Commun.* , 2013, **49**, 6840–6842.